PHYSICAL REVIEW B VOLUME 5, NUMBER 3 1 FEBRUARY 1972

Frequency Dependence of the Josephson Current*†

C. A. Hamilton‡§
Department of Electrical Engineering, University of Rochester, Rochester, New York 14627
(Received 22 June 1971)

Careful measurements have been made of the power and frequency dependence of the ac Josephson steps in a superconducting tunnel junction exposed to 20–26-GHz microwave radiation. At values of $2\alpha = 2eV_{rf}/hf > 25$, significant deviations from Bessel-function behavior $[J_N(2\alpha)]$ begin to occur. These deviations are caused by a sharp peak in the Josephson current at a frequency $f_J = 4\Delta/h$, i.e., the Riedel peak. The experimental data are used to measure the shape of this peak. Simultaneous measurements of the Josephson and quasiparticle effects are also presented. These results demonstrate that the two effects have the theoretically predicted correlation. Our experiments as a whole demonstrate the theory of superconducting tunnel junctions to be on very firm experimental ground.

I. INTRODUCTION

In a previous communication[1] we showed that careful measurements of the amplitudes of the ac Josephson steps can be used to demonstrate the existence of a sharp peak in the Josephson current at a frequency of $4\Delta/h$, i.e., the Riedel peak.[2] In this paper we expand on this work and present new and more complete information on (i) the frequency dependence of the Josephson step amplitudes, (ii) the relationship between step-amplitude data and the frequency dependence of the Josephson current $I_J(f_J)$, (iii) inherent limitations on the observability of $I_J(f_J)$, (iv) the experimental details, and (v) the correlation between the Josephson effects and the rf-induced quasiparticle effects.

The conventional analysis of the ac Josephson effect begins with Josephson's[3] first two equations for the current in a superconducting tunnel junction:

$$I = I_1 \sin\phi \ , \tag{1}$$

$$\frac{d\phi}{dt} = \frac{2eV}{\hbar} \ . \tag{2}$$

If the junction is placed in a microwave field at a frequency f, the voltage across it has an rf component and is written

$$V = V_{dc} + V_{rf}\cos 2\pi ft \ . \tag{3}$$

Equations (1)–(3) can be combined to show that in the presence of an rf field, the junction current has a dc component which is given by[4]

$$I_{dc}(V_{dc}) = I_J(0)\sum_N |J_N(2\alpha)|\,\delta(V_{dc} \pm Nhf/2e) \ , \tag{4}$$

where $\alpha = eV_{rf}/hf$, $\delta(x) = 0$ for $x \neq 0$, $\delta(x) = 1$ for $x = 0$, and J_N is the Nth-order Bessel function. Equation (4) predicts a series of constant-voltage steps in the I-V curve at the discrete voltages given by $Nhf/2e$. The amplitude of the Nth step is predicted to vary as the Nth-order Bessel function. The existence of these steps and the Bessel-function oscillation of their amplitudes have been reported in a number of papers.[4,5]

Implicit in the derivation of Eq. (4) is the assumption that the Josephson current amplitude is independent of frequency. Riedel,[2] however, has shown that the Josephson current $[I_J(f_J)]$ has a frequency dependence which peaks very sharply at a Josephson frequency $f_J = 2eV/h$, corresponding to the superconducting energy gap, i.e., at a bias voltage $V_{dc} = 2\Delta/e$. The result for the case of two identical superconductors at $T = 0\,^{\circ}\mathrm{K}$ is given by

$$I_J(f_J) = (\Delta/eR)K(hf_J/4\Delta) \ , \qquad hf_J/4\Delta \leq 1$$
$$= (\Delta/eR)(4\Delta/hf_J)K(4\Delta/hf_J) \ , \qquad hf_J/4\Delta \geq 1 \tag{5}$$

where K is a complete elliptic integral of the first kind and R is the normal tunneling resistance. Equation (5) assumes an isotropic gap and does not include the effects of quasiparticle damping. Figure 1 is a graph of $I_J(f_J)$.

Werthamer[6] has shown that the frequency dependence of I_J modifies the behavior of the Josephson step amplitudes. An outline of the details of this analysis is given in the Appendix. The final result is

$$I_{dc}(V_{dc}) = \sum_N \left|\sum_n J_n(\alpha)J_{N-n}(\alpha)I_J((2n-N)f)\right| \times \delta(V_{dc} \pm Nhf/2e) \ . \tag{6}$$

If the value of α is small, the n summation in Eq. (6) converges before the value of I_J changes significantly from $I_J(0)$. Using this fact together with the identity[7]

$$\sum_n J_n(\alpha)J_{N-n}(\alpha) = J_N(2\alpha) \ , \tag{7}$$

we see that Eqs. (4) and (6) are nearly identical. Thus, for small values of V_{rf}, the step amplitudes

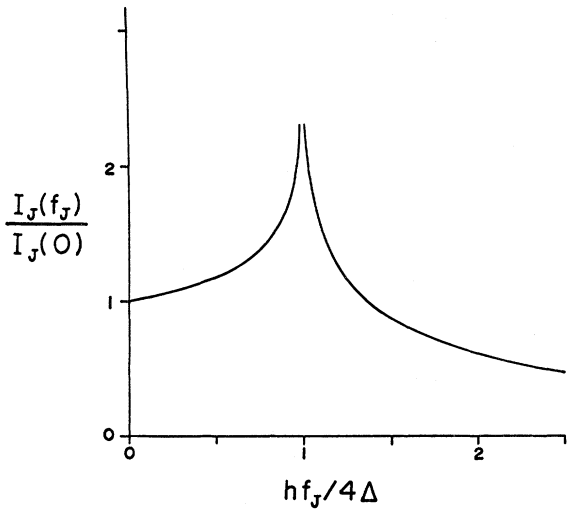

FIG. 1. Josephson current I_J as a function of Josephson frequency f_J.

show the normal Bessel-function behavior. For large values of V_{rf}, harmonics of the applied radiation interact with the enhanced Josephson current near the peak and significant deviations from Bessel-function behavior occur. An experimental investigation of these deviations provides a method for demonstrating the existence of the Riedel peak. Further, by making such measurements over a range of frequency, the height and shape of the peak can be determined.

Our experiment, although involving a number of practical problems, used a basically straightforward approach to obtain these data. A very-small-area tin-oxide-tin tunnel junction was mounted in a waveguide. A large number of I-V curves were then recorded as a function of the applied microwave power. The amplitudes of the ac Josephson steps as recorded in these I-V curves were then compared with the predictions of the theory. Our data agree well with both the rf voltage and frequency dependence of Eq. (6). We also show how these results are used to obtain data on the shape of $I_J(f_J)$. This analysis indicates that the technique employed in our experiments can be used to determine $I_J(f_J)$ only in a small region near the peak.

The Werthamer analysis outlined in the Appendix also derives an expression for the quasiparticle current in the presence of an rf field.[8] This component of the junction current is given by

$$I_{dc}(V_{dc}) = \sum_n J_n^2(\alpha) I_0(V_{dc} + nhf/e) , \qquad (8)$$

where $I_0(V_{dc})$ is the quasiparticle current with no applied rf. Since I_0 has a sharp step in current at $V_{dc} = 2\Delta/e$, Eq. (8) predicts that, in the presence of an rf field, the I-V curve will have a series of steps at the voltages $2\Delta/e \pm nhf/e$. These are the "photon-assisted tunneling steps" first observed by Dayem and Martin.[9] After some controversy,[10,11] the $J_n^2(\alpha)$ rf voltage dependence of these steps has recently been verified.[12,13] Since both these quasiparticle steps and the ac Josephson steps are directly related in the theory to the same value of V_{rf}, a comparison of the two effects in the same junction is of interest. We have made such simultaneous measurements and found that both effects can be fit to the theory using a common V_{rf} scale.

In Sec. II we describe our experimental procedures and the problems associated with junction fabrication and data recording. In Sec. III data are presented to demonstrate the correlation between the Josephson effects and the quasiparticle effects. The frequency dependence of the Josephson step amplitudes and the resulting determination of $I_J(f_J)$ is the subject of Sec. IV. Our results are summarized and compared to other related work in Sec. V.

II. EXPERIMENTAL PROCEDURES

The assumption of a spatially uniform rf field [Eq. (3)] is basic to the theoretical analysis. Thus, in order to observe the theoretically predicted step-amplitude variation, it is essential to make junctions in which the rf field is reasonably constant. Since the wave velocity in the junction is considerably less than the free-space velocity,[14] the junction dimensions must be very much smaller than the free-space wavelength.

Our experiments were performed at a frequency of 20–26 GHz and employed up to four tin-oxide-tin thin-film junctions on a $0.25 \times 0.50 \times 0.01$ in. sapphire substrate. The very small junctions required were fabricated using the in-line point-overlap configuration.[12,15] In this configuration, the tip of a sharply pointed strip of tin just barely overlapped the edge of the second thin film. Junctions made in this way had an approximately triangular shape with areas on the order of 10^{-6} cm^2. The details of the vacuum-evaporation procedure are given in Ref. 12.

After removing the junctions from the vacuum system, leads were attached and the substrate was mounted perpendicular to the E field in a K-band (0.420×0.170 in.) waveguide. The substrate and its microwave mounting were immersed directly in the liquid helium. At the top of the cryostat, the waveguide was connected through a frequency meter and a precision attenuator to a reflex klystron. The junction I-V curves were displayed on an x-y oscilloscope using the conventional four-wire connection with a constant current drive.

Extensive shielding was used to prevent any undesirable disturbance of the junction. The inner

helium Dewar was surrounded with a copper shield and the outer nitrogen Dewar was surrounded with two layers of high-permeability molypermalloy magnetic shielding. In addition, the entire experiment was performed within a double-layer shielded room.

In spite of all this shielding, electrical disturbances associated with the experiment itself frequently caused the junctions to trap magnetic flux. Since this trapped flux produced irreversible changes in the I-V curve, it was very detrimental to the experimental measurements. It was therefore necessary to record the large amount of data required in a very short time and with a minimum of electrical disturbance. This was accomplished by taking a motion picture of the I-V curve (as displayed on the oscilloscope) as the rf power was continuously varied. Thus, in 20 sec, I-V curves could be recorded for each of more than 300 values of the applied rf power. The precision attenuator reading was projected into the right-hand side of the picture and was thus recorded on each frame of the movie film.

The data were reduced by examining the film frame by frame. The Josephson steps appeared as vertical lines with well-defined ends. The lengths of these lines were thus a good measure of the step amplitudes. The quasiparticle step amplitudes were measured by taking the vertical distance at the step voltage between tangent lines to the I-V curve just above and below the step. The attenuator reading A (in dB) was converted to the value for the rf voltage across the junction (V_{rf}) using the relation

$$V_{rf} = C10^{-A/20} \quad . \tag{9}$$

The constant C was chosen for a best fit to the theory.

Figure 2 shows a typical junction I-V curve with

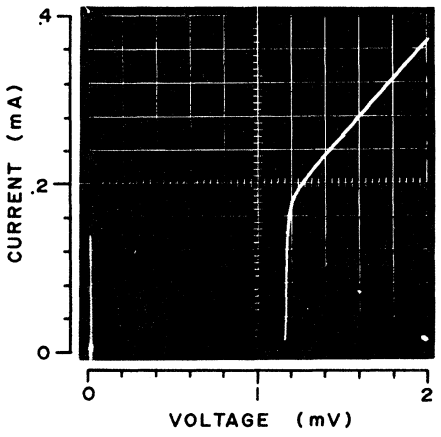

FIG. 2. Oscilloscope trace of the I-V curve for a typical 5.4-Ω superconducting tin-oxide-tin junction.

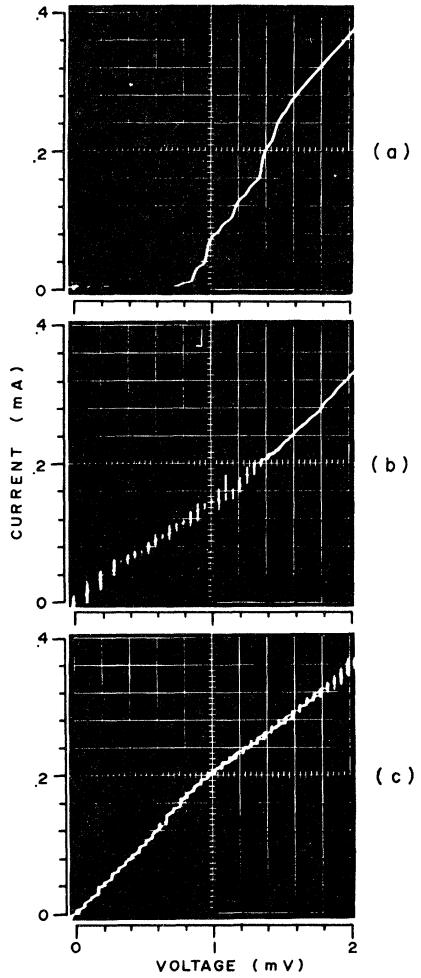

FIG. 3. I-V curves with applied radiation at 25 GHz and (a) $V_{rf} \simeq 0.3\,(2\Delta/e)$, (b) $V_{rf} \simeq 2\Delta/e$, and (c) $V_{rf} \simeq 1.5\,(2\Delta/e)$.

$V_{rf} = 0$. The junction resistance ($R \simeq 5.4\ \Omega$) is measured from the slope of the curve at voltages well above the gap voltage $2\Delta/e$. The lack of any significant current at lower voltages is an indication of the absence of microshorts or other nontunneling processes. The dc Josephson current (spike at zero voltage) is about 80% of the maximum theoretical value of $\pi\Delta/2eR$. The effect of the constant current drive is also clear from the switching points at $V = 0$ and at the limit of the dc Josephson current.

In the frequency range of our experiment (20–26 GHz), and for small values of V_{rf}, the Josephson steps were strongly overlapped. That is, at a given current, the voltage could be at any one of a number of the values $Nhf/2e$. Thus the voltage was not a single-valued function of the current and with our constant current bias, the Josephson steps could not all appear in the I-V curve. At higher

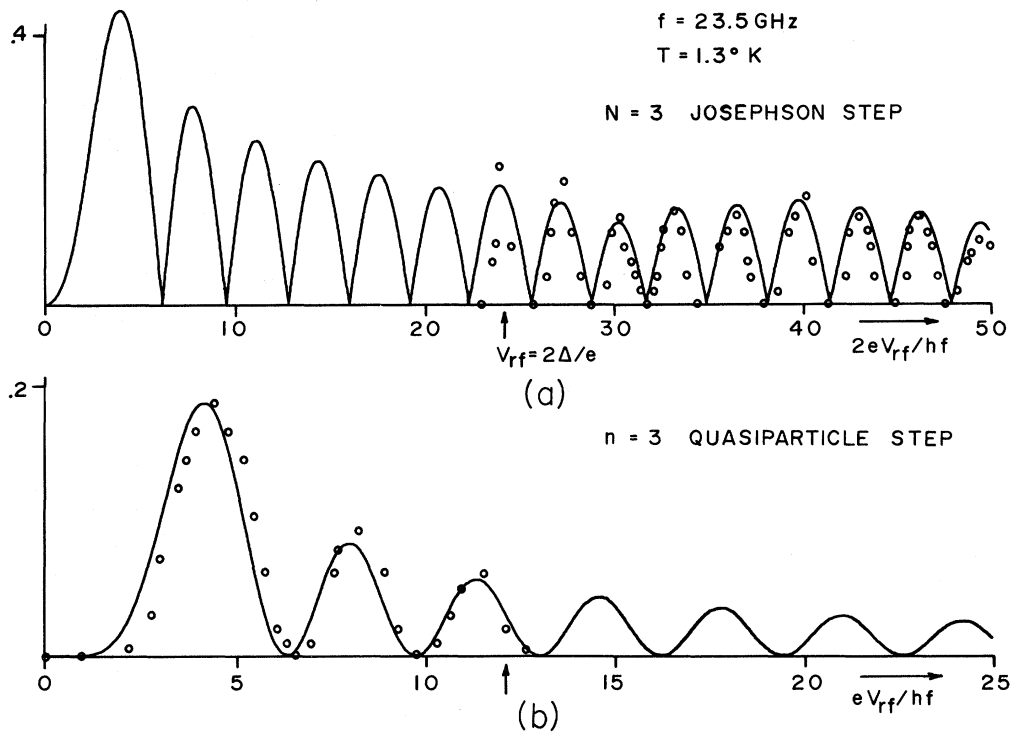

FIG. 4. Experiment and theory compared for the $N=3$ Josephson and quasiparticle steps.

values of V_{rf}, the amplitudes of the Josephson steps decreased and the background quasiparticle current increased so that the voltage eventually became a single-valued function of the current.

Figure 3 shows how the I-V curve behaved as the applied rf power increased. In Fig. 3(a), $V_{rf} \simeq 0.3(2\Delta/e)$. No Josephson steps are observed because they cannot be traced out by the constant current drive. Several quasiparticle steps, which comprise the background current, are visible in the region around $V_{dc} = 2\Delta/e$. In Fig. 3(b), $V_{rf} \simeq 2\Delta/e$ and many Josephson steps are observable. There are still, however, switching regions indicating some overlap of the Josephson steps. In Fig. 3(c), $V_{rf} \simeq 1.5(2\Delta/e)$ and the I-V curve has a staircaselike form. For the lower steps this curve is single valued everywhere and the full oscillations of the Josephson steps are measurable.

This behavior of the I-V curve in our experiment put limits on the observability of both the Josephson steps and the quasiparticle steps. The quasiparticle steps could be measured for values of V_{rf} from zero up to about $2\Delta/e$. For significantly larger values of V_{rf}, the quasiparticle steps were obscured by the Josephson steps and their amplitudes became too small to measure. For the case of the Josephson steps, the situation was just the opposite. Their amplitudes could be measured only for values of $V_{rf} > 2\Delta/e$. In the region near $2\Delta/e$, overlapping of the steps may have resulted in incorrect measurements although we believe that the maxima were generally observed properly.

III. CORRELATION OF THE JOSEPHSON AND QUASIPARTICLE EFFECTS IN SMALL JUNCTIONS

In our measurements of the Josephson step amplitudes we determined only the relative value of V_{rf}. Thus the comparison of experimental and theoretical values of V_{rf} involves an arbitrary constant. Simultaneous measurements of the quasiparticle steps provide another measure of this constant and thus a further test of the theory.

A typical result of many such measurements is shown in Fig. 4. The solid curve in Fig. 4(a) is the theoretical amplitude variation for the $N=3$ Josephson step as computed from Eq. (6). As a result of the Riedel peak, this theoretical curve has a small deviation from the usual phenomenologic result $|J_N(2\alpha)|$. This effect is discussed in detail in Sec. IV. The solid curve in Fig. 3(b) is the theoretical amplitude variation for the $n=3$ quasiparticle step. [From Eq. (8) this is just $J_3^2(\alpha)$.]

Our measured step-amplitude data points are shown for both effects. These data were divided by a normalization constant which was chosen to

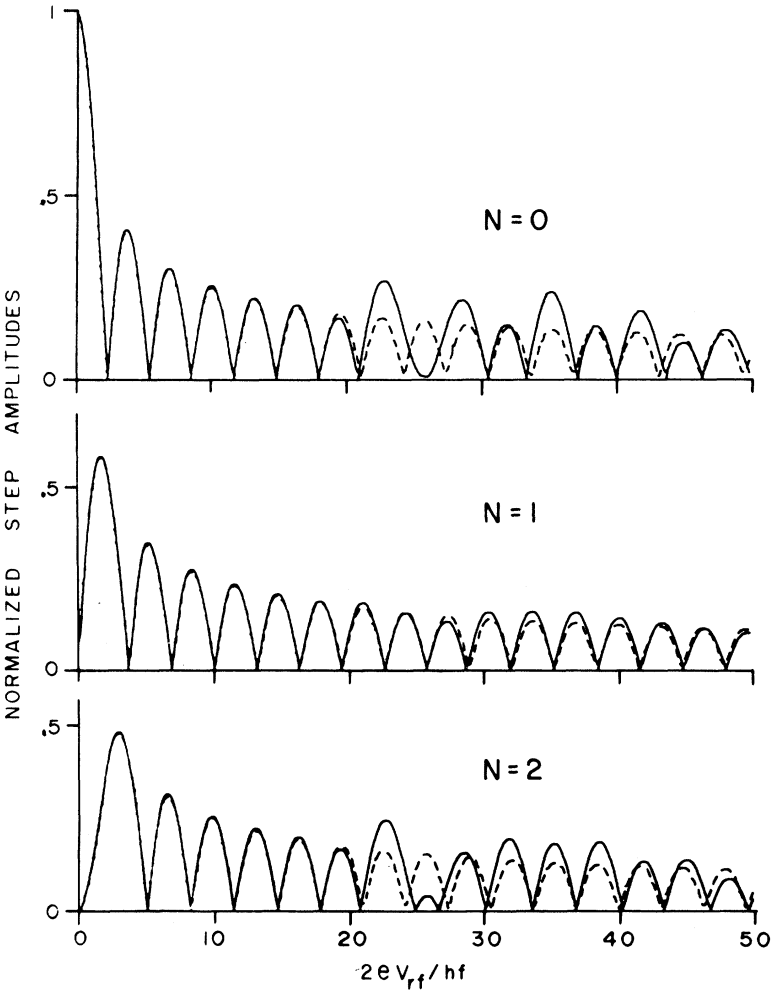

FIG. 5. Theoretical Josephson step amplitudes from Eq. (4) (dashed lines) and Eq. (6) (solid lines). The frequency is 25.7 GHz.

obtain a best fit to the theoretical curves. In each case this constant was approximately (±10%) the amplitude of the zero-order step with $V_{rf} = 0$. The V_{rf} scale for these data is the same for both the Josephson steps and the quasiparticle steps, i.e., just one value of C in Eq. (9). The fact that the periodicity of the data closely matches the theory in both cases demonstrates that the magnitude of V_{rf} may be treated the same way for both effects. Thus, the predicted factor-of-2 difference in the arguments of $|J_N|$ for the Josephson step amplitudes and of J_n^2 for the quasiparticle step amplitudes is correct within our experimental error of about 5%.

A similar result has been observed at 73 GHz by Longacre and Shapiro[13] in experiments with point-contact junctions.

In contrast to these results, Sweet and Rochlin[16] have made a comparison of the Josephson and quasiparticle effects at 3.9 GHz and have reported poor agreement with the theory. However, their comparison was based only on the first zero of the zero-voltage Josephson current. Our data suggest that this may not be a reliable test of the theory.

IV. FREQUENCY DEPENDENCE OF JOSEPHSON CURRENT

A. Theoretical Predictions

In Sec. I, we pointed out that deviations from Bessel-function behavior in the Josephson step amplitudes are observed only when V_{rf} is large. To put this on a more quantitative basis we note that the frequency dependence of I_J has an important effect in Eq. (6) only when there are significant terms in the n summation for which the argument of I_J approaches the peak, i.e., $(2n - N)f \geq 4\Delta/h$. These terms correspond to the integer values $n \geq 2\Delta/hf + \frac{1}{2}N$. Using the property of Bessel functions that $J_n(\alpha) \simeq 0$ for all $|n| > \alpha$, it follows that the significant terms in the n summation of Eq. (6) are those for which $|n| \leq \alpha$. The effect of the peak in I_J will thus be observed first when $\alpha \geq |n| \simeq 2\Delta/hf + \frac{1}{2}N$. If the Mth Josephson step

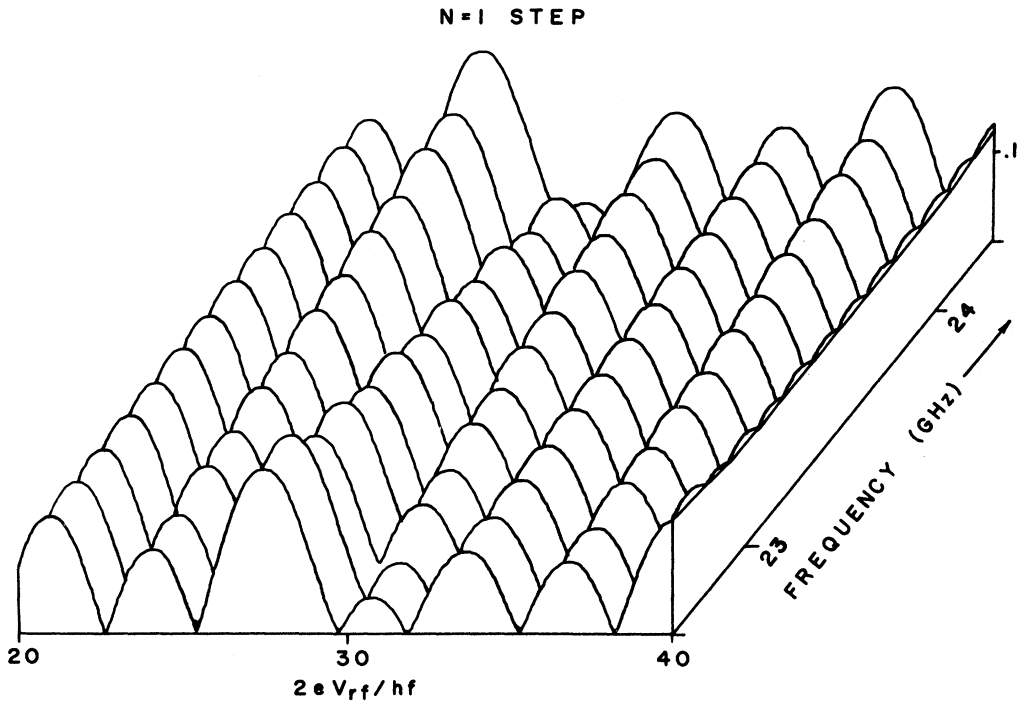

FIG. 6. Three-dimensional plot showing the theoretical frequency dependence of the $N=1$ Josephson step amplitude.

falls near the gap ($Mhf/2e \simeq 2\Delta/e$), this becomes

$$2\alpha = 2eV_{rf}/hf \gtrsim N+M \quad . \tag{10}$$

This is an approximate rule for the value of V_{rf} at which the first deviation from $|J_N(2\alpha)|$ behavior occurs.

From Fig. 1 and Eq. (6) it is seen that these deviations will be most pronounced when $(2n-N)f \simeq 4\Delta/h$, i.e., when one of the Josephson steps falls very near the gap voltage. If an even-numbered step falls near the gap (M even), this condition can be satisfied only for N even and thus the even-numbered steps show the strongest deviations. A frequency shift sufficient to bring an adjacent odd-numbered step in line with the gap shifts the strongest deviations to the odd steps. The existence of these unusually large and highly frequency-dependent deviations is a direct consequence of the sharp peak in $I_J(f_J)$.

Figure 5 is a plot of the theoretical variation for the $N=0-2$ step amplitudes with applied radiation at 25.7 GHz ($2\Delta/e$ is taken as 1.175 meV). At this frequency, the 22nd Josephson step falls near the gap ($M=22$). The dashed lines are the values of $|J_N(2\alpha)|$. The solid lines are computed from Eq. (6). The accuracy of the "sum rule" [Eq. (10)] is apparent in these curves. For instance, the solid and dashed curves should first diverge for the $N=0$ step at a value of $2\alpha = N+M = 22$. It is also apparent that the largest deviations occur in the even-numbered steps. This is expected because M is even.

The pattern of deviations shown in Fig. 5 is highly frequency dependent. This frequency dependence for the $N=1$ step is depicted in the three-dimensional graph of Fig. 6. The frequency scale of 22.4–24.4 GHz corresponds to a variation in the number of steps to the gap from 25 to 23. Thus, at either end of the frequency axis there are an odd number of steps to the gap and since N is odd, large deviations occur. The center region around 23.4 GHz corresponds to 24 steps to the gap and there are no large deviations. As expected from the sum rule, the first large deviation moves down the $2eV_{rf}/hf$ axis as the frequency increases.

B. Experimental Data

In Fig. 7 we have expanded the curves of Fig. 5 in the region $2\alpha = 20-45$ and compared these theoretical curves with a corresponding set of our experimental data. In assessing these data it is important to observe the relative change in amplitude from one maximum to the next. On this basis the data are in good agreement with Eq. (6) (solid line) and clearly show the influence of the peak in $I_J(f_J)$. Figure 7 also shows that the decline in successive maxima is more rapid in the experiment than in the theory. The severity of this effect was found to increase with junction size and is probably the result of a slight spatial variation of the rf field.[17]

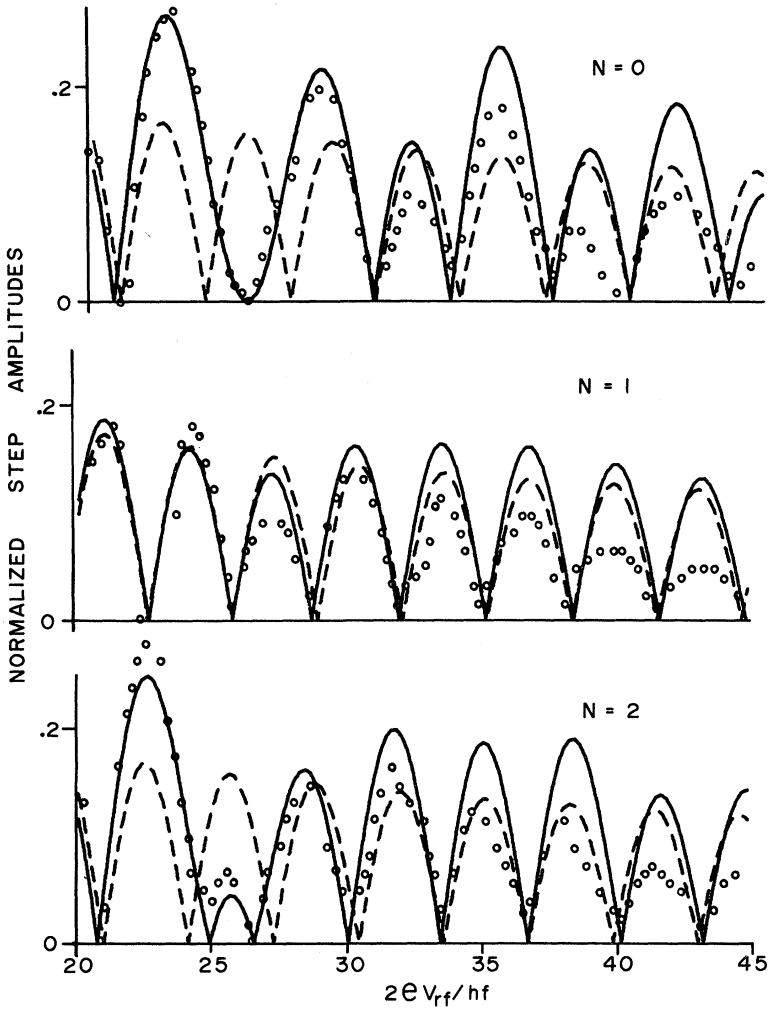

FIG. 7. Josephson step amplitudes from Eq. (4) (dashed lines), Eq. (6) (solid lines), and experimental data points (open circles). The frequency is 25.7 GHz.

The data points in Fig. 7 are typical of our results for all nine of the steps measured.

An alternative method of displaying the data is to fix the value of N and α at a particular maximum of $I_{dc}(\alpha)$ and plot step amplitude as a function of frequency. In the three-dimensional picture of Fig. 6 this corresponds to a slice parallel to the end rather than parallel to the front. Figure 8 is such a plot. The values $N=0$, $2\alpha = 25.9$ and $N=1$, $2\alpha = 24.4$ are chosen because these numbers result in theoretical curves with a particularly strong frequency dependence. As before, the solid lines are computed from Eq. (6) (without the absolute-value operation) and the dashed lines are the value of $J_N(2\alpha)$. The singularities in the theoretical curves are a direct result of the singularity in $I_J(f_J)$.

The data points (open circles) are obtained from a series of curves like Fig. 7 as a function of frequency. Since every point on the curves of Fig. 8 corresponds to a maximum as a function of α, it is not necessary to make an accurate measurement of the rf voltage. Rather, at each frequency, we locate the proper range of α in the experimental data and choose the nearest maximum value of the step amplitude. As before, the step amplitudes are multiplied by a single constant chosen to obtain a best over-all fit. Figure 8 demonstrates that the data do have a strong frequency dependence and that this frequency dependence is in fairly good agreement with theory.

C. Shape of Riedel Peak

Data like those shown in Fig. 8 can be used to determine the shape of the Riedel peak. Our experiment and the mathematics of Eq. (6) put certain restrictions on such a determination. We begin with a discussion of these restrictions.

In Eq. (6), the Riedel peak function $I_J((2n-N)f)$ can be thought of as a weighting function for the terms in the n summation of Eq. (7). In order to understand how the variation of I_J affects the final

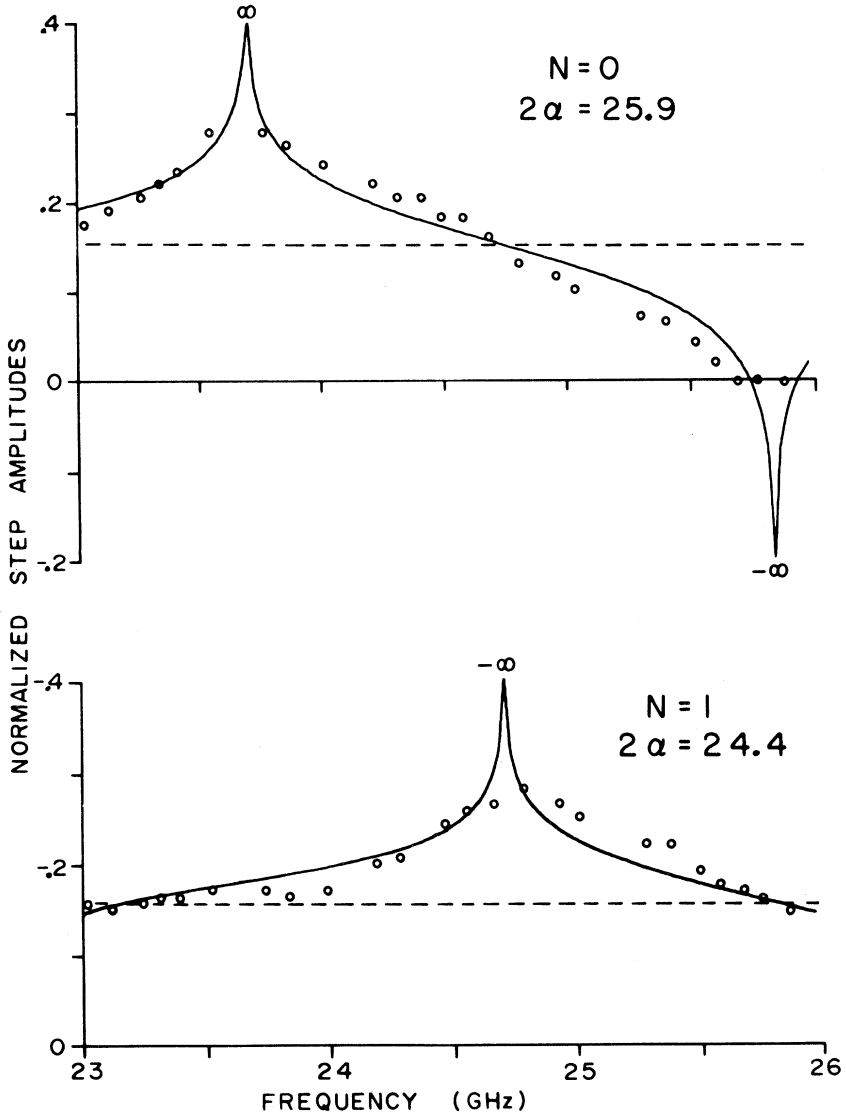

FIG. 8. Frequency dependence of the Josephson step amplitude for N and 2α fixed from Eq. (4) (dashed line), Eq. (6) (solid line), and experimental data points (open circles).

result it is very helpful to examine the convergence of this n summation. Thus, in Fig. 9(a), we have chosen the values $N=0$ and $\alpha=35$ and plotted the left side of Eq. (7) as a function of the number of terms in the summation. The figure shows that the principal contribution comes from the first few terms. Although the terms for $6<n<35$ may have large values, their net contribution over a range of n tends to cancel out. As expected, there is essentially zero contribution from terms for which $n>\alpha$. The behavior shown in Fig. 9(a) is typical of the convergence of Eq. (7) for all values of n and α.

Figure 9(b) is a graph of the function $I_J((2n-N)f)$ using the same n scale and a value of $f=23.5$ which is typical for our experiment. As described above, this curve is the weighting function for each term in the summation.

A comparison of Figs. 9(a) and 9(b) suggests an important conclusion. Since the $1/f_J$ decay of $I_J(f_J)$ for $n>15$ is relatively smooth with respect to the oscillations of Fig. 9(a), this falloff of I_J has very little effect on the final result in Eq. (6). Thus, our experiment cannot yield data about the shape of $I_J(f_J)$ except near $f_J=4\Delta/h$.

The fact that several researchers have observed the $|J_N(2\alpha)|$ step-amplitude variation for values of $V_{rf}\ll 2\Delta/e$ [4,5] is, in effect, a verification of the flat region in $I_J(f_J)$, where $f_J\ll 4\Delta/h$. Our conclusions about the observability of $I_J(f_J)$ are summarized as follows: (a) For $f_J\ll 4\Delta/h$ previous results have shown that $I_J\simeq$ const; (b) for $f_J\simeq 4\Delta/h$ the shape of I_J is observable in our experiment; and (c) for $f_J>4\Delta/h$ the shape of I_J is not observable in our experiment.

In the region near the peak, the magnitude of

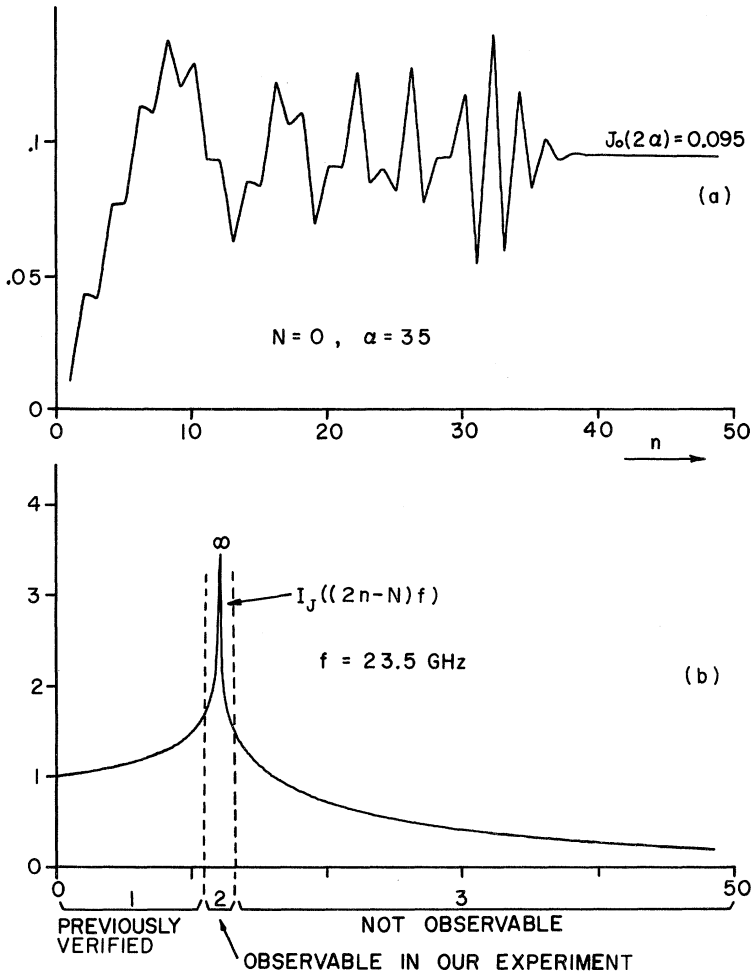

FIG. 9. (a) Plot of the convergence of Eq. (7) as a function of the number of terms in the sum and (b) the Riedel peak function which modulates the amplitudes of these terms in Eq. (6).

I_J in Eq. (6) is changing very rapidly from one term to the next and its effect does not cancel out. At the frequency of our experiment, the two terms for which $(2n-N)f \simeq \pm 4\Delta/h$ produce the major deviations from the $|J_N(2\alpha)|$ behavior. Denote these terms by n' and n'' such that $f_J' = (2n'-N)f = -(2n''-N)f \simeq 4\Delta/h$. Solving Eq. (6) for $I_J(f_J')$, the result is

$$I_J(f_J') = \Big(I_e(N, \alpha, f) - \sum_{\substack{n \\ n\neq n' \\ n\neq n''}} J_n(\alpha) J_{N-n}(\alpha) I_J((2n-N)f) \Big) \Big/ [J_{n'}(\alpha) J_{N-n'}(\alpha) + J_{n''}(\alpha) J_{N-n''}(\alpha)], \quad (11)$$

where $I_e(N, \alpha, f)$ is the experimentally measured step amplitude. In the numerator of Eq. (11), I_J is taken as the theoretical value given in Eq. (5). We are thus assuming the theoretical value of I_J everywhere except near the peak. This assumption is reasonable because (i) the constant region below the peak has been verified in previous experiments and (ii) as long as I_J is fairly smooth in the region above the peak, it has very little effect on the final result. By using experimental data $I_e(N, \alpha, f)$ over a range of frequency around f_c, Eq. (11) yields data on $I_J(f_J)$ for the region $4\Delta/h - f_c < f_J < 4\Delta/h + f_c$.

If I_e has some fixed experimental error, then the resulting error in I_J is minimized by choosing N and α to maximize the denominator of Eq. (11). This is equivalent to choosing the data at values of N and α for which there is a maximum deviation from the $J_N(2\alpha)$ curve.

A series of points computed from Eq. (11) is plotted in Fig. 10. The step-amplitude data used in this computation come from the same data set plotted in Fig. (8) and use the same scaling factors. The points shown as open circles are computed using the experimental measurements for the $N = 0$ step amplitude at a value of $2\alpha = 25.9$. The points shown as squares are for $N = 2$ and $2\alpha = 25.8$. These measurement points correspond to regions of maximum deviation from the $J_N(2\alpha)$ curve. In

both cases the frequency range is 23–26 GHz and the temperature is 1 °K. The solid line is the theoretical value of $I_J(f_J)$ and is computed from Eq. (5). The data show that the peak is slightly broadened and that it attains a maximum value of about 3.0.

The rounding of the singularity can be attributed to gap anisotropy and quasiparticle damping. If one assumes a simple triangular distribution of the gap, a spread of only about 1% produces the rounding which we observe. Scalapino and Wu[18] assume that for the case of thin-film junctions gap anisotropy is negligible. They analyze the effects of damping in terms of an imaginary gap parameter Δ_2. A comparison of our data with their result suggests that the ratio Δ_2/Δ is about 10^{-3}.

V. CONCLUSIONS

We have made detailed measurements of the frequency and rf voltage dependence of the ac Josephson step amplitudes. These measurements which extend to values of $V_{rf} > 4\Delta/e$ are in good agreement with the theory and clearly show the effects of a sharp peak in the Josephson current. This peak occurs at a frequency corresponding to the superconducting energy gap $f_J = 4\Delta/h$. An analysis of the predictions of the theory shows how our measurements can be used to determine the shape of the peak. Our data on tin-oxide-tin junctions at 1 °K suggest a current peak height about three times the value of the zero-voltage current.

A number of papers have presented experimental results related to the frequency dependence of the Josephson current. McDonald *et al.*[19] have performed experiments which demonstrate the existence of Josephson phenomena at frequencies well above the gap. They have observed the 110th harmonic of a 70-GHz applied signal, as well as the direct effect of applied radiation at 2500 GHz. These results do not provide quantitative data on the frequency dependence of I_J but certainly support the rather gradual fall off predicted in the theory.

Several researchers[20,21] have reported the existence of structure at $V = 2\Delta/ne$, $n = 1, 2, \ldots$ in the I-V curves of Josephson junctions. Werthamer[6] has suggested that this structure is caused by the sharp peak in I_J. The experimental results of Giaever and Zeller support this conclusion. However, some controversy still remains in the explanation of this effect.

Buckner and Finnegan[22] have recently made a series of measurements of the zero-voltage Josephson current in tin-oxide-tin junctions which were exposed to radiation at 140 GHz. In their experi-

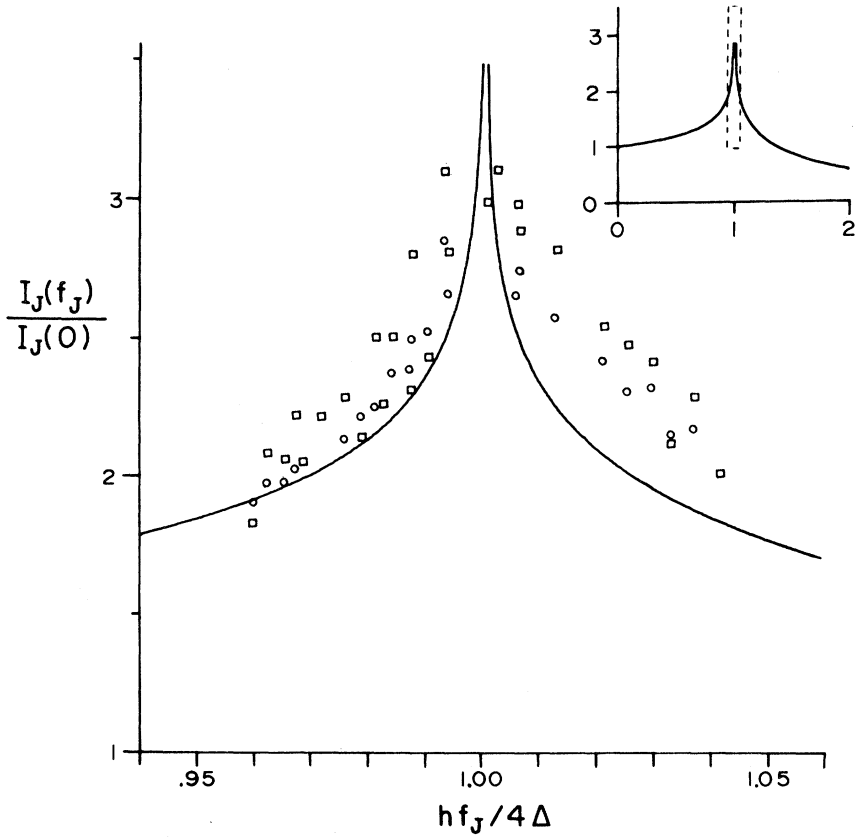

FIG. 10. Riedel peak function $I_J(f_J)$ (solid line) and data (points) computed from experimental measurements of the Josephson step amplitudes. The dashed box in the insert shows the region plotted.

ment, V_{rf} and f are fixed and the gap is adjusted (via the temperature) in the region near $hf \simeq \Delta(T)$. For certain values of V_{rf}, their $N=0$ step-amplitude data are sharply peaked at $hf=\Delta(T)$. This result is also a demonstration of the existence of the Riedel peak.

Summing up, in our experiments, the sharp peak in the Josephson current and its effect on the ac Josephson step amplitudes have been demonstrated and found to be in excellent agreement with theory.

ACKNOWLEDGMENTS

The author is much indebted to Sidney Shapiro and Andrew Longacre, Jr. for many helpful discussions and suggestions.

APPENDIX

We indicate here the principal steps in the Werthamer analysis which lead to Eq. (6). The calculation is for the special case of a junction made of identical superconductors with no dc magnetic field. We begin with Werthamer's Eq. (7) for the total current flowing in a non-self-coupled junction with a spatially homogeneous potential difference:

$$I(t)=\frac{-2e}{\hbar^2}\,\mathrm{Re}\sum_{kq}\int_{-\infty}^{t}d\bar{t}\;e^{n\bar{t}/\hbar}\int_{-\infty}^{\infty}dE_1\,dE_2\,e^{-(i/\hbar)(E_1-E_2)(\bar{t}-t)}[f(E_1)-f(E_2)]$$

$$\times\left[\,|T_{k,q}|^2A_k(E_1)A_q(E_2)\,e^{(i/2)[\phi(t)-\phi(\bar{t})]}+T_{k,q}T_{-k,-q}\bar{B}_k(E_2)B_q(E_1)\,e^{(i/2)[\phi(t)+\phi(\bar{t})]}\right]\ . \qquad (12)$$

$T_{k,q}$ is the tunneling matrix element connecting state k on one side of the junction with state q on the other side. It is assumed to be constant. The Fermi function f is

$$f(E)=(e^{-E/kT}+1)^{-1}\ . \qquad (13)$$

The spectral weight functions $A_k(E)$ and $B_k(E)$ are given by

$$A_k(E)=\tfrac{1}{2}[(1+\epsilon_k/E_k)\delta(E-E_k)+(1-\epsilon_k/E_k)\delta(E+E_k)]\ ,$$

$$B_k(E)=-\tfrac{1}{2}i\{(\Delta/E_k)[\delta(E-E_k)-\delta(E+E_k)]\}\ , \qquad (14)$$

$$\bar{B}_k(E)=(\Delta^*/\Delta)B_k(E)\ ,$$

where $E_k=(\epsilon_k^2+\Delta^2)^{1/2}$, $\epsilon_k=\hbar^2k^2/2m$, and $\eta=0^+$. Equation (2) determines the time dependence of ϕ. Thus, with a voltage across the junction given by Eq. (3), the phase is

$$\phi(t)=(2eV_{dc}t/\hbar)-(2eV_{rf}/hf)\sin 2\pi ft\ . \qquad (15)$$

Now perform the following steps on Eq. (12): (a) Substitute Eq. (15) into terms involving ϕ. (b) Use the identity

$$e^{-ix\sin\theta}=\textstyle\sum_n J_n(x)\,e^{-in\theta}$$

to remove sine terms in the exponentials. (c) Perform the trivial $\bar{t}$ integration. The result is

$$I(t)=\mathrm{Im}\textstyle\sum_n\sum_{n'}J_nJ_{n'}\{e^{-i(n-n')2\pi ft}\,j_1(n'hf-eV_{dc})$$

$$+\exp[-i(n+n')2\pi ft+i2eV_{dc}t/\hbar+i\sigma]$$

$$\times\,j_2(-n'hf+eV_{dc})\}\ , \qquad (16)$$

where $\alpha=eV_{rf}/hf$ and the current amplitudes j_1 and j_2 are defined by

$$j_1(E)=\frac{-2e}{\hbar}\sum_{kq}\int_{-\infty}^{\infty}dE_1\,dE_2\,[f(E_1)-f(E_2)]\,|T_{k,q}|^2$$

$$\times\,A_k(E_1)A_q(E_2)(E_1-E_2-E+i\eta)^{-1}$$

and

$$e^{i\sigma}j_2(E)=\frac{-2e}{\hbar}\sum_{kq}\int_{-\infty}^{\infty}dE_1\,dE_2\,[f(E_1)-f(E_2)]\,T_{k,q}$$

$$\times\,T_{-k,-q}\bar{B}_k(E_2)B_q(E_1)[E_1-E_2-E+i\eta]^{-1}\ . \qquad (17)$$

The first term of Eq. (16) is the quasiparticle current and has a dc component when $n=n'$. If we let $N=n+n'$, then the second term has a dc component only at the discrete voltages given by $Nhf=2eV_{dc}$. These are the voltages of the Josephson steps. We choose the phase $\sigma=\pm\frac{1}{2}\pi$ to maximize the current on each step because it is this maximum current which is observed in the dc I-V curve. The dc component of current then is

$$I_{dc}(V_{dc})=\sum_n J_n^2(\alpha)\,\mathrm{Im}J_1[nhf-eV_{dc}]+\sum_{N\geq 0}\Big|\sum_n J_n(\alpha)$$

$$\times J_{N-n}(\alpha)\,\mathrm{Re}j_2[(n-\tfrac{1}{2}N)hf]\Big|\,\delta(V_{dc}\pm Nhf/2e)\ . \qquad (18)$$

$\mathrm{Im}j_1$ is just the normal electron tunnel current without applied radiation. Converting to our notation $\mathrm{Im}j_1(E/e)=I_0(V_{dc})$. Using $E=eV_{dc}=\frac{1}{2}hf_J$ we see that $\mathrm{Re}j_2$ is the frequency dependence of the Josephson current. In our notation this is $I_J(f_J)$, and its value is given in Eq. (5).

*Based in part on a thesis submitted for the degree Ph.D. in Electrical Engineering (University of Rochester, New York, 1971) (unpublished).

†Supported by the National Science Foundation under Grant No. GK 10562.

‡Fannie and John Hertz Predoctoral Fellow.

§Present address: National Bureau of Standards, Boulder, Colo.

[1]C. A. Hamilton and Sidney Shapiro, Phys. Rev. Letters 26, 426 (1971).

[2]E. Riedel, Z. Naturforsch. 19a, 1634 (1964).

[3]B. D. Josephson, Phys. Letters 1, 251 (1962); Rev. Mod. Phys. 36, 216 (1964); Advan. Phys. 14, 419 (1965).

[4]S. Shapiro, A. R. Janus, and S. Holly, Rev. Mod. Phys. 36, 223 (1964).

[5]C. C. Grimes and Sidney Shapiro, Phys. Rev. 169, 397 (1968).

[6]N. R. Werthamer, Phys. Rev. 147, 255 (1966).

[7]M. Abramowitz and I. Stegun, *Handbook of Mathematical Functions* (Dover, New York, 1965), Eq. 9.1.75.

[8]The result given in Eq. (8) was first derived by P. K. Tien and J. P. Gordon, Phys. Rev. 129, 647 (1963).

[9]A. H. Dayem and R. J. Martin, Phys. Rev. Letters 8, 246 (1962).

[10]C. F. Cook and G. E. Everett, Phys. Rev. 159, 374 (1967).

[11]S. Teller and B. Kofoed, Solid State Commun. 8, 235 (1970).

[12]C. A. Hamilton and Sidney Shapiro, Phys. Rev. B 2, 4494 (1970).

[13]Andrew Longacre, Jr. and Sidney Shapiro, Bull. Am. Phys. Soc. 16, 399 (1971).

[14]J. C. Swihart, J. Appl. Phys. 32, 461 (1961).

[15]S. A. Buckner, J. T. Chen, and D. N. Langenberg, Phys. Rev. Letters 25, 738 (1970).

[16]J. N. Sweet and G. I. Rochlin, Phys. Rev. B 2, 656 (1970).

[17]We have made an analysis of the spatial-variation problem for the Josephson steps similar to that discussed in Ref. 12 for the quasiparticle steps. This analysis suggests that when the spatial variation becomes significant ($\Delta\alpha \simeq 3$), only the highest steps ($N \simeq 2\alpha$) should be observed. This result is consistent with our experimental data.

[18]D. J. Scalapino and T. M. Wu, Phys. Rev. Letters 17, 315 (1966).

[19]D. G. McDonald, V. E. Kose, K. M. Evenson, J. S. Wells, and J. D. Cupp, Appl. Phys. Letters 15, 121 (1969); D. G. McDonald, K. M. Evenson, J. S. Wells, and J. D. Cupp, J. Appl. Phys. 42, 179 (1971).

[20]I. Giaever and H. R. Zeller, Phys. Rev. B 1, 4278 (1971).

[21]J. M. Rowell and W. L. Feldman, Phys. Rev. 172, 393 (1968).

[22]S. A. Buckner and T. F. Finnegan, Bull. Am. Phys. Soc. 16, 399 (1971).

PHYSICAL REVIEW B VOLUME 5, NUMBER 3 1 FEBRUARY 1972

Pair Propagator Approach to Fluctuation-Induced Diamagnetism in Superconductors–Effects of Impurities

Patrick A. Lee and Marvin G. Payne*

Department of Physics, Yale University, New Haven, Connecticut 06520

(Received 14 May 1971; revised manuscript received 22 July 1971)

We have obtained, within the ladder approximation, expressions for the electron pair propagator of a dilute superconducting alloy (i.e., subject to the condition $\omega_D\tau \gg 1$) in the presence of strong magnetic field and above the transition temperature. We then proceed to calculate microscopically the free energy and the magnetization. The procedure used in an earlier work on pure superconductors is justified, but important additional contributions are found for alloys.

I. INTRODUCTION

Recently, Gollub, Beasley, and Tinkham[1] (GBT) reported observation of universal behavior in the fluctuation-induced diamagnetism of superconductors above the transition temperature. Owing to the fact that fluctuations of very short wavelength contribute to the diamagnetism, the data deviate markedly from the calculation by Prange[2] which is exact within the framework of the Ginsburg-Landau (GL) theory. Patton, Ambegaokar, and Wilkins[3] (PAW) have attempted to deal with the problem by introducing an *ad hoc* cutoff energy E into the fluctuation spectrum. However, it is found that the parameter E required to fit the experimental data for clean materials is about ten times smaller than expected from physical arguments.[1] In a recent work[4] (hereafter referred to as I) we pointed out that for pure samples in the presence of a strong magnetic field the usual replacement $\vec{q} \to \vec{q} + 2e\vec{A}/c$ assumed by previous authors is no longer valid. We calculated the mag-

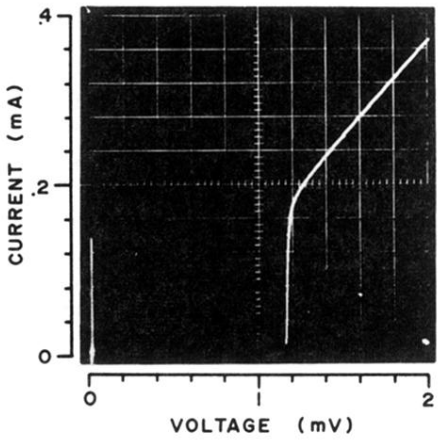

FIG. 2. Oscilloscope trace of the I-V curve for a typical 5.4-Ω superconducting tin-oxide-tin junction.

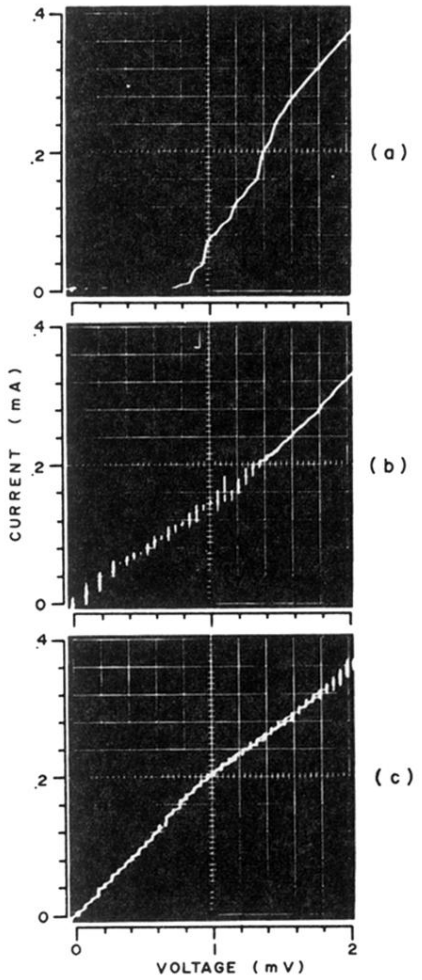

FIG. 3. I–V curves with applied radiation at 25 GHz and (a) $V_{rf} \simeq 0.3\,(2\Delta/e)$, (b) $V_{rf} \simeq 2\Delta/e$, and (c) $V_{rf} \simeq 1.5\,(2\Delta/e)$.